A Neutron Reflectivity Study of Poly(*N*-isopropylacrylamide) at the Air−Water Interface with and without Sodium Dodecyl Sulfate

Robert M. Richardson,[†] Robert Pelton,*[,‡] Terence Cosgrove,[†] and Ju Zhang[‡]

School of Chemistry, Bristol University, Cantock's Close, Bristol, BS8 1TS, UK, and McMaster Centre for Pulp and Paper Research, Department of Chemical Engineering, McMaster University, Hamilton, Ontario, Canada L8S 4L7

Received January 20, 2000; Revised Manuscript Received May 5, 2000

ABSTRACT: The properties of poly(*N*-isopropylacrylamide) (polyNIPAM) at the air/water interface, with and without sodium dodecyl sulfate (SDS), were measured by neutron reflectivity and surface tension. Below the lower critical solution temperature (LCST), polyNIPAM adsorbs at the air/water interface to give a thin ($\delta \sim 1.5$ nm) layer with a low water content approximately equal to phase-separated polyNIPAM above the LCST. Above the LCST the adsorbed polymer layer increases by a factor of 10 approximately equal to the effective diameter of a single phase-separated polymer chain (a globule). Polymer-bound SDS lowers the density of adsorbed polyNIPAM because of electrostatic effects.

Introduction

Temperature-sensitive polymers are a route to "intelligent materials" with applications in drug release and separations.[1] The recent literature contains many papers describing the properties of aqueous poly(*N*-isopropylacrylamide) (polyNIPAM) which has a lower critical solution temperature (LCST) of 32 °C.[2] PolyNIPAM's temperature sensitivity originates from the interactions of water with pendant isopropyl groups. In contrast to the behavior of polyacrylamide, polyNIPAM tends to adsorb onto solids and at the air/water interface to lower surface tension.

Fujishige et al.[3] used the Whilhelmy method to measure surface tension for 0.25−1% w/v PNIPAM which gave surface tension values of 47.8 mJ/m^2 at 31 °C compared with 41.9 mJ/m^2 at an unspecified temperature above the LCST. We confirmed that the surface tension of the aqueous solution did not decrease much with temperature in the range 20−40 °C even though polymer in solution experienced a phase transition at 32 °C.[4] Thus, surface tension seems to be one property of aqueous polyNIPAM which does not display significant temperature sensitivity. In subsequent work we have reported extensive experimental studies of surface dynamic surface tension behaviors both below and above the LCST.[5] Surface tension was not sensitive to polyNIPAM molecular weight and concentration, and the temperature dependency of surface tension was not much greater than that of water alone. On the other hand, the kinetics of surface tension lowering reflecting the polymer adsorption kinetics was sensitive to temperature and polyNIPAM concentration. Higher concentrations and temperatures below the LCST gave the fastest surface tension decrease on newly formed surfaces. Below and above the LCST the surface tension of a freshly formed interface approaches a steady-state value in a classical S-shaped curve when surface tension is plotted against the logarithm of time. The shape of the curve can be fitted with the empirical Hua Rosen equation.[6] On the other hand, attempts to employ less arbitrary mass transport models including the Van Eijk and Cohen Stuart[7] models were unsuccessful at predicting the time scale for surface tension lowering as a function of the initial concentration of polyNIPAM. This was explained by proposing that the rearrangement of polymer at the air/water interface was the rate-controlling phenomenon.[8]

Novel, oscillating pendant drop experiments were employed to probe the dynamics of surface rearrangement. In this technique, the surface area of a pendant drop was changed sinusoidally by a factor of 2, and the resulting surface tension fluctuations were measured. Although the surface area excursions were large (i.e., a factor of 2), the corresponding surface tensions oscillations were only a few mJ/m^2. This was explained by fast loop-to-train transitions when the surface was expanded. Although many aspects of the surface tension results are fascinating, they give limited insight into the structure of polyNIPAM at the air/water interface.

The first attempt to characterize the structure of polyNIPAM at the air/water interface was by Kawaguchi and co-workers,[9] who spread PNIPAM on a Langmuir trough and used ellipsometry to measure surface concentration and adsorbed layer thickness as functions of surface pressure. At 16 °C the maximum surface coverage was about 1 mg/m^2, and this amount was nearly doubled when the experiment was conducted at 31 °C. In a subsequent study at 16 °C they reported coverage of about 2 mg/m^2 and an ellipsometric thickness of about 6.5 nm. These values correspond to an average polymer volume fraction in the adsorbed layer of about 30%.[10] One of the goals of this work is to extend our knowledge of the structure of polyNIPAM at the air/water interface by neutron reflectivity measurements.

The solution properties of polyNIPAM are also sensitive to the presence of surfactants. Following the work of Eliassaf,[11] Schild and others have shown that both cationic and anionic surfactants bind to aqueous polyNIPAM generally forming a complex which is more hydrophilic.[12,13] We have characterized SDS binding to cross-linked, water-swollen uniform polyNIPAM microgels.[14] The gels offer two advantages: they can be centrifuged which, in turn, permits measurement of

[†] Bristol University.
[‡] McMaster University.
* To whom correspondence should be addressed. E-mail peltonrh@mcmaster.ca.

10.1021/ma000095p CCC: $19.00
Published on Web 08/22/2000

Table 1. Steady-State Surface Tensions for 50 mg/L PolyNIPAM Solutions

polymer	temp (°C)	surface tension (mJ/m^2)	T^* (s)
polyNIPAM-D7	25	46.6	40
polyNIPAM-D7	40	40.1	187
polyNIPAM-H [5]	25	43.1	6
polyNIPAM-H	40	40.2	2090

surfactant binding isotherms. Second, microgel swelling is easily monitored by dynamic light scattering which shows that SDS binding causes significant increases in microgel swelling. Recently, we employed neutron scattering to probe the structure of bound SDS in polyNIPAM microgels.[15] In contrast to the behavior of SDS binding to poly(ethylene oxide),[16] the bound surfactant is present in small domains containing five or less surfactant molecules.

Nothing has been published about the influence of SDS on the properties of polyNIPAM at the air/water interface. In this work we also use neutron reflectivity to probe the interfacial properties of SDS/polyNIPAM mixtures.

In summary, polyNIPAM provides an interesting temperature-sensitive system which may give insight into the behavior of more complex molecules at the air/water interface. Important unresolved issues include a detailed description of polyNIPAM at the air/water interface both below and above the LCST in an effort to understand why surface tension is so insensitive to temperature. Additionally, SDS binding is relevant to many potential applications of polyNIPAM, and thus it is of interest to understand how SDS influences the adsorbed layer structure. In this work, we present a detailed description of the adsorbed polymer based on neutron reflectivity measurements. PolyNIPAM based on deuterated isopropane was investigated in solutions of nonreflecting H_2O/D_2O mixtures.

Experimental Section

Two polyNIPAM polymers were used. PolyNIPAM-H was prepared in our laboratory with $M_w = 5.47 \times 10^5$ and $M_w/M_n = 1.8$.[5] PolyNIPAM-D7, based on deuterated propane, was purchased from Polymer Source, Dorval, QU, Canada. According to the supplier, polyNIPAM-D7 had a $M_n = 358\,000$, $M_w/M_n = 2.6$, and $[\eta]$ in methanol was 0.905 dL/g. BDH SDS was used without further purification.

The surface tension of 50 ppm of polyNIPAM-D7 solutions in null reflecting water, H_2O:D_2O (92:8 vol:vol), was measured by an automated pendant drop technique in Neumann's laboratory at the University of Toronto.[17] The surface tension of mixtures of polyNIPAM L-6B and SDS was measured by the Du Noüy method. The measurements were made in a thermostated cell after a minimum of 20 min equilibration time.

The neutron reflection experiments were made using the NG7 reflectometer at the NIST Center for Neutron Research, Gaithersburg, MD. The solutions were contained in a PTFE trough that was enclosed by a temperature-controlled environmental box which has been described in detail elsewhere.[18]

Results

Aqueous PolyNIPAM. The surface tension of 50 ppm of polyNIPAM-D7, $M_n = 358\,000$, dissolved in a 8:92 by volume mixture of D_2O:H_2O (null reflecting water) was measured at two temperatures, and the results are compared with those for aqueous polyNIPAM-H in Table 1. The surface tension for both polymers was 40 mJ/m^2 at 40 °C whereas at 25 °C polyNIPAM-H gave a slightly lower (3 mJ/m^2) surface tension than observed for polyNIPAM-D7. In both cases surface tension was not very temperature dependent over the range spanning the LCST. Also shown in Table 1 are the t^* values which are the times required to observe $^1/_2$ the maximum surface tension change. In both cases the transport of polymer to the interface was much slower above the LCST where the polymer was present as phase-separated particles.

Neutron reflectivity measurements were made from two solutions with different neutron scattering contrasts between the polyNIPAM and the water at 25 and 44 °C. The measurements from polyNIPAM-D7 in null reflecting water and polyNIPAM-H in null reflecting water give complementary information, which allowed a detailed picture of the interfacial structure to be established at 25 and 44 °C. The transitions induced by temperature variation and SDS addition were then followed using polyNIPAM-D7 in null reflecting water only.

Neutron reflection from polyNIPAM-D7 in D_2O is sensitive to the amount and thickness of the adsorbed layer of polyNIPAM but is completely insensitive to its position relative to the surface of the water. The polyNIPAM-H layer in D_2O reduces the scattering length density near the surface, and so the reflectivity from this contrast is sensitive to the distance of the polyNIPAM layer from the water surface. To extract this information, the reflectivity results from polyNIPAM-D7 in null reflecting water and polyNIPAM-H in D_2O were fitted simultaneously with the reflectivities calculated from the same distribution of water and NIPAM.

The model scattering length density profiles, $\rho(z)$, were calculated from the equation

$$\rho(z) = b_P n_P(z) + b_W n_W(z)$$

In this equation b_W is the average scattering length for a water molecule (0 for null water and 19.1×10^{-5} Å for D_2O), and b_P is the scattering length for a polyNIPAM segment (90.5×10^{-5} Å for polyNIPAM-D7 and 24.3×10^{-5} Å for polyNIPAM-H). The $n_W(z)$ is the number density of water which has been modeled as a simple error-function profile at the interface. The term $n_P(z)$ is the number density of polyNIPAM segments which has been modeled as a uniform slab with error-function profiles at its upper and lower boundaries.

$$n_W(z) = \frac{n_W^*}{2}\{1 + \mathrm{erf}(\alpha,\sigma_W)\}$$

$$n_P(z) = \frac{n_P^*}{2}\{(1 + \mathrm{erf}(\alpha + \beta, \sigma_U)) - (1 + \mathrm{erf}(\alpha + \beta + \delta, \sigma_L))\}$$

where $\mathrm{erf}(\alpha,\sigma)$ is an error function centered at α and with width parameter σ. The parameter α is the distance of the water surface from the arbitrary origin and was fixed at 10 Å in this work, β is the position of the polyNIPAM boundary relative to the water surface, and δ is the thickness of the polyNIPAM slab. The parameter σ characterizes the sharpness of the boundaries that the error functions represent. These functional forms were chosen for simplicity in order to introduce the minimum number of parameters. The parameters n_W^* and n_P^* are the maximum number densities of water molecules and polyNIPAM segments, respectively. The reflectivity for the two combinations

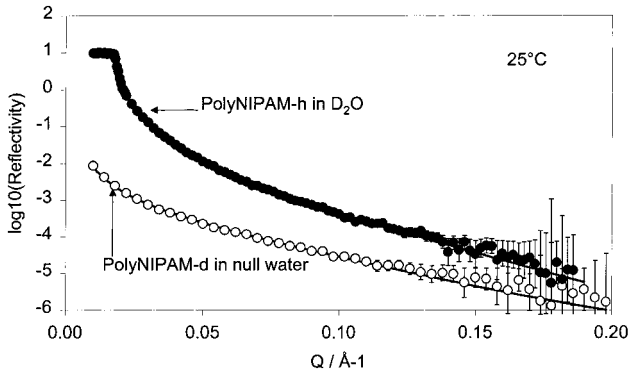

Figure 1. The reflectivity of polyNIPAM-d7 in null reflecting water (open points) and polyNIPAM-h in D2O (closed points) at 25 °C. Note, the polyNIPAM-h in D2O results are shifted up 1 unit for clarity. The lines are the best simultaneous fit to the two measured reflectivities. The points represent the experimental data and the lines were predicted by simultaneous fitting of both data sets.

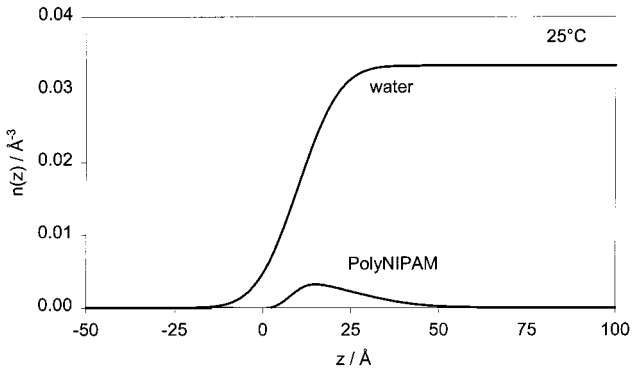

Figure 2. Number density distributions corresponding to the fits in Figure 1.

of contrasts was calculated from the two $\rho(z)$ profiles using the optical matrix method[19] with the appropriate values of b_W and b_P. The calculated reflectivities were then fitted to those experimentally measured by varying parameters. For the water molecule distribution, the width of the water−air interface (σ_W) was varied, but the maximum number density of water (n_W^*) was fixed at the value for bulk water (0.033 Å^{-3}). For the polyNIPAM segment distribution, the maximum number density (n_P^*), the slab thickness (δ), the widths of the upper and lower boundaries (σ_U and σ_L), and relative position (β) of the slab were varied. The reflectivity versus Q plots for both polymer solvent contrasts at 25 °C are shown in Figure 1. The lines are the best simultaneous fit to the two measured reflectivities, and the corresponding segment number densities are shown in Figure 2. Since neat polyNIPAM has a segment number density of 0.0054 Å^{-3} the results in Figure 2 confirm that the polyNIPAM forms a thin but fairly high volume fraction (∼0.6) layer just beneath the water surface.

On heating to 44 °C polyNIPAM phase separates. The reflectivity curves are shown in Figure 3, and the corresponding number densities are shown in Figure 4. The thickness of the layer increases, and its segment number density approaches that of neat polyNIPAM. However, this simultaneous modeling of both contrasts suggests that there is a significant amount of the polyNIPAM layer above the water surface.

The temperature dependence of the polyNIPAM layer was followed by neutron reflection from the polyNIPAM-

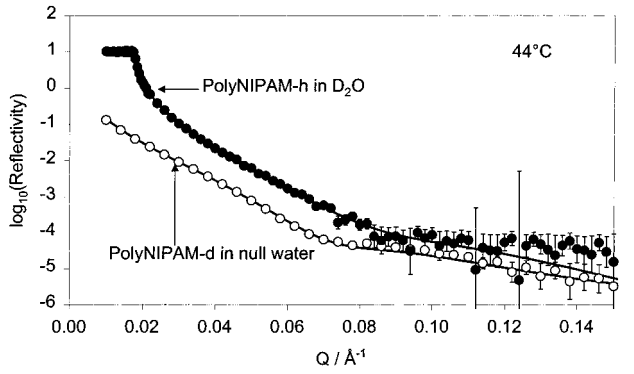

Figure 3. The reflectivity of polyNIPAM-d7 in null reflecting water (open points) and polyNIPAM-h in D2O (closed points) at 44 °C. Note, the polyNIPAM-h in D2O results are shifted up 1 unit for clarity. The lines are the best simultaneous fit to the two measured reflectivities.

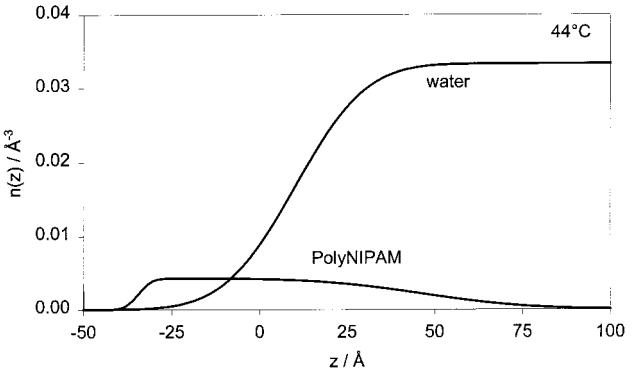

Figure 4. Number density distributions corresponding to the fits in Figure 3.

D7 in null reflecting water. The reflectivity was analyzed by fitting with the single uniform slab model. Since $b_W = 0$, there are only four relevant parameters: the thickness of the layer, δ, the maximum number density of polyNIPAM (n_P^*), and the width of the upper and lower interfaces, σ_U and σ_L. The scattering length density profile for the solution in null water is then given by the formula

$$\rho(z) = \frac{b_P n_P^*}{2}\{(1 + \mathrm{erf}(\alpha,\sigma_U)) - (1 + \mathrm{erf}(\alpha + \delta, \sigma_L))\}$$

The absorbed amount Γ may be calculated from these parameters using the equation

$$\Gamma = n_P^* \delta$$

It was not possible to determine all four parameters uniquely from the weaker reflectivity profiles (i.e., those from lower temperatures) so the boundary width parameters were fixed for these. However, the values of Γ were always insensitive to these parameters and were well-defined by the fits. For additional confirmation, the reflectivity was analyzed by determining the low-Q slope of "Guinier" type plots of $\ln(RQ^2)$ vs Q^2. This method makes no assumptions about the shape of the number density profile, and it yielded the same values of Γ within experimental error.

The thickness and absorbed amount determined from the fits are shown Figure 5 as functions of temperature for a 50 ppm solution. Below 32 °C, the LCST for polyNIPAM, the coverage was 1.5 mg/m^2 with a corre-

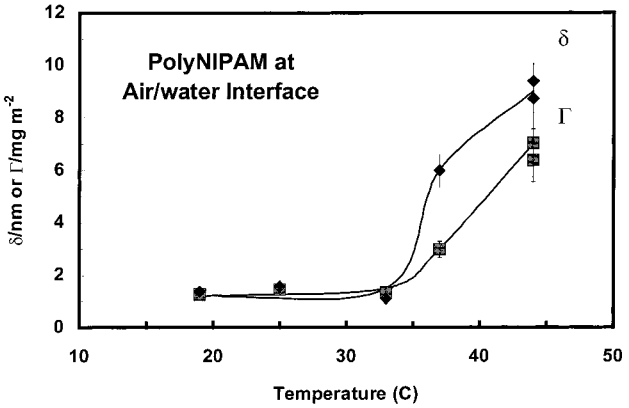

Figure 5. The mass and thickness of the polyNIPAM layer at the air/water interface as functions of the temperature.

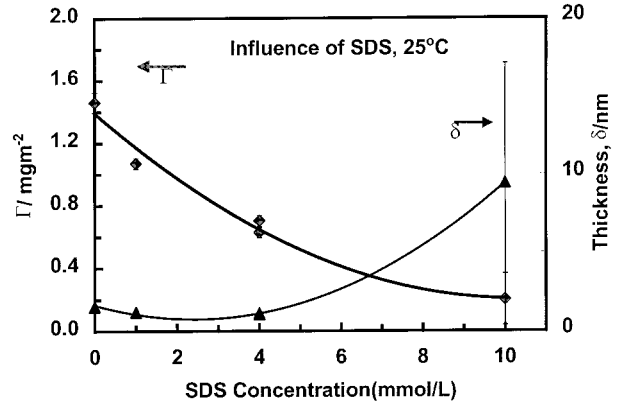

Figure 6. The influence of SDS on the properties of polyNIPAM at the air/water interface. Measurements were made with polyNIPAM-D7 in null reflecting water and SDS in the proton form.

sponding thickness of 1.5 nm. Furthermore, these values seem insensitive to temperature over the range 19−32 °C. Above 32 °C the amount of adsorbed polymer and the thickness of the layer increased by a factor of 8 at 44 °C.

Aqueous SDS + PolyNIPAM. SDS binds to polyNIPAM. Previous neutron results with polyNIPAM microgels have shown that the bound surfactant is present in small aggregates containing less than five surfactant molecules,[15] and recent NMR studies reveal that molecular motion of polyNIPAM-bound SDS is similar to that of SDS in free micelles.[20] Figure 6 shows the adsorbed amount of polyNIPAM-D7 obtained by fitting a slab model to the neutron reflectivity results from deuterated NIPAM with added SDS. The SDS does not contribute significantly to the reflectivity because it has a low scattering length compared to the deuterated polymer. The addition of SDS caused a dramatic decrease in polyNIPAM adsorption at the air/water interface. At high surfactant concentration the reflected intensities were low give a great uncertainty in thickness estimates.

SDS binding reduces the mass of adsorbed polymer per square meter of interface, Γ, but induces a modest increase in adsorbed layer thickness, δ, up to at least 4 mmol/L SDS. The absence of a large layer expansion at low SDS concentrations was a surprise since both polyNIPAM microgels,[14] and linear chains in solutions display large expansions with SDS binding. On the other hand, the thickness values are similar to those of

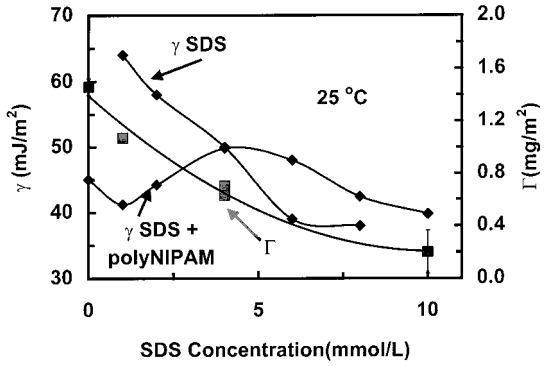

Figure 7. The comparison of surface tension and reflectivity results as functions of SDS concentration. γSDS = surface tension of SDS solutions; γSDS+polyNIPAM = surface tension of 50 mg/L polyNIPAM plus SDS; ΓSDS+polyNIPAM = surface coverage of polymer measured by reflectivity.

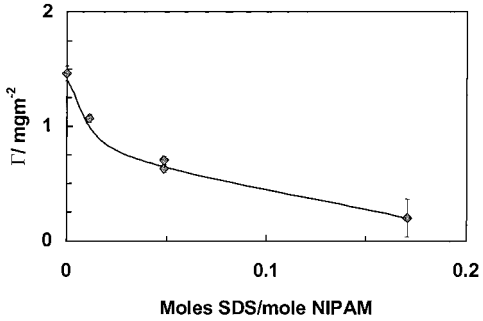

Figure 8. The adsorbed concentration of polyNIPAM as a function of the amount of polymer bound SDS estimated from ref 15.

deuterated SDS in the presence of poly(vinylpyrrolidone).[21]

Figure 7 compares surface tension results as a function of SDS concentration with and without polyNIPAM-H at 25 °C. In the presence of polymer the surface tension actually increases to give a maximum at an SDS concentration of about 4 mmol/L—with higher SDS concentrations the surface tension decreases to a limiting value similar to that in the absence of polyNIPAM. Also shown in Figure 7 is the amount of adsorbed polyNIPAM-D7 as a function of SDS concentration (i.e., the same results shown in Figure 6). From 1 to 4 mmol/L SDS where the surface tension was increasing, the amount of adsorbed polyNIPAM was decreasing. Previous work has shown that surface tension is rather insensitive to polyNIPAM microgel molecular weight.[4] Therefore, in comparing these results, we assume that the surface tension behavior of polyNIPAM-H reflects the behavior of polyNIPAM-D7 since the two differ by only a factor of 1.5 in molecular weight.

Previously, we have reported the binding isotherm of SDS to cross-linked polyNIPAM microgels.[15] Since most of the microgel properties reflect the properties of linear polyNIPAM, it seems reasonable to apply our binding isotherm to the present results. A mole balance analysis reveals that less than 1% of the added SDS is bound to polyNIPAM because the polymer concentration is low (50 mg/L). Figure 8 shows the surface concentration of polyNIPAM, measured by reflectivity, as a function of the average number of moles of bound SDS molecules per NIPAM repeating unit. The surface concentration of polyNIPAM was reduced by a factor of 2 when the amount of bound surfactant was 0.04 mol of SDS per

mole of isopropyl groups. PolyNIPAM adsorption was nearly eliminated when the amount of bound SDS was 0.17 mol/mol. Therefore, SDS binding renders polyNIPAM less surface active, presumably because of the introduction of charge groups. This result is consistent with the observation that both linear polyNIPAM chains and polyNIPAM microgel particles expand with SDS binding.[14]

Discussion

Below the LCST, the neutron reflectivity data indicate that polyNIPAM forms an unusually dense (volume fraction $\sim$ 0.6), thin (δ = 1.5 nm) layer. The volume fraction of polymer in the interfacial layer is less than that of phase-separated polyNIPAM above the LCST[2] but is higher than normally observed for homopolymers physically adsorbed onto solids.[22]

On the basis of the light scattering results of Kobuta et al.,[23] the radius of gyration of poly(*N*-isopropylacrylamide) at 25 °C is given by $R_g = KM_w^v$ where $K = 0.011$ nm and $v = 0.591$. On the basis of this relationship, the radius of gyration of polyNIPAM-D7 is 21 nm, which is an order of magnitude greater than the adsorbed layer thickness.

If we consider the cross section of a polyNIPAM perpendicular to the vinyl carbon−carbon bond axis, there are three domains. The *N*-isopropyl groups are the most hydrophobic, the methylene chain forming the backbone is the next most hydrophobic, whereas the domain around the amide group is the most hydrophilic. On organizing these three chain subunits at the air−water interface, it seems reasonable to propose that the units next to air will have the isopropyl groups facing if not protruding into it. The isopropyl groups on the two interior layers, however, are likely to associate with each other. This would lead to a surface structure in which both the hydrophobic and hydrophilic parts minimize their interactions with their respective incompatible phases and lead to a rather flattened surface structure. This behavior is similar to that found with random copolymer at the oil−water interface.[24]

The polyNIPAM concentration in the adsorbed layer was high and approximately equal to the polymer concentration in phase-separated polyNIPAM above the LCST. Thus, adsorption in this case could be viewed as a surface-induced phase separation. That is, the release of structured water around the isopropyl groups phase drives phase separation at the interface. If true, this suggests that there could be a surface phase separation temperature which is lower than the LCST for the solution.

Kawaguchi and co-workers have reported ellipsometric measurements for 600 000 molecular weight polyNIPAM at the air/water interface at 16 °C.[10] Their adsorbed layer thickness values were about 7.0 nm, which is 5 times greater than our value. Furthermore, their coverage values were 2.5 mg/m^2, which is nearly twice our value. Conversion of Kawaguchi's data to a density of polyNIPAM in the surface layer gives a value of 0.36 g/mL; our corresponding value is about 1 g/mL. Therefore, the published ellipsometry data for 16 °C suggest a much more extended adsorbed layer than do the reflectivity results at 16 °C. The reason for this discrepancy is not known.

Above the LCST the polyNIPAM surface layer is much thicker, suggesting that phase-separated polymer in solution deposits onto the interface. A single polymer coil as a collapsed sphere above the LCST will be 11 nm in diameter, assuming that the phase-separated polymer is 20% water. This value is close to the layer thickness observed at 44 °C (see Figure 5). In the solution, phase-separated polyNIPAM is usually present as stable colloidal particles with diameters around 500 nm, which is very much larger than the adsorbed layer thickness. Therefore, it seems that individual phase-separated polymer chains deposited onto the surface before the larger colloidally stable particles could reach the surface or that, upon adsorption, the large colloidal particles broke apart to give a layer of individual phase-separated chains.

A finding of this work is that surface tension is not a good predictor of the total amount of polymer at the air/water interface. From 25 to 40 °C the surface tension *decreased* only 6 mJ/m^2 whereas the amount of adsorbed polymer *increased* by a factor of 7. Presumably surface tension is sensitive to only the first few angstroms of the interface, and thus surface tension is a measure of the concentration of segments in trains and short loops. Furthermore, in our opinion the concentration of adsorbed segments of phase-separated polymer is not very sensitive to temperature or polymer concentration.

The general features of the SDS results seem consistent with previous data. Surfactant effectively binds sulfate chains onto polyNIPAM, making it more hydrophilic which, in turn, drives the polymer from the interface giving an increase in surface tension (see Figure 7). Surfactant binding did not give a significant increase in the polyNIPAM adsorbed layer thickness. Instead, the number of surface chains decreased with increased binding.

A related publication from Cabane's group appeared after this paper was completed.[25] That work described neutron reflectivity measurements with protonated polyNIPAM in water/D_2O mixtures. Although reflectivity measurements from their inverse system (i.e., protonated instead of deuterated polyNIPAM) are intrinsically less sensitive, their main results and interpretations are in accord with ours. However, subtle differences do exist. We observed a more abrupt onset of layer thickening with increasing temperature. Also, at low temperature we observed more poly(*N*-isopropylacrylamide) at the interface, which is consistent with our use of a higher molecular weight. The fact that we used deuterated polyNIPAM with contrast matched water means our adsorbed amounts are not dependent upon any assumed model of polymer distribution at the interface.

Conclusions

1. Below the LCST polyNIPAM adsorbs at the air/water interface to give a thin ($\delta \sim 1.5$ nm) layer with a low water content approximately equal to phase-separated polyNIPAM above the LCST.

2. Above the LCST the thickness of the adsorbed polymer layer is about 10 times greater than at room temperature. The layer thickness above the LCST approximately corresponds to the diameter of individual phase-separated polyNIPAM chains (i.e., a globule) with 20 wt % bound water.

3. Polymer-bound SDS lowers the mass of adsorbed polyNIPAM because of electrostatic effects.

Acknowledgment. The authors acknowledge Prof. W. Neumann for use of his surface tension apparatus and Dr. Ling Yang for some surface tension measure-

ments. Also acknowledged are Sushil Satija and Lipiin Sung for help with the use of the neutron facilities at NIST.

References and Notes

(1) Osada, Y.; Ross-Murphy, S. *Sci. Am.* **1993**, *May*, 82.
(2) Schild, H. G. *Prog. Polym. Sci.* **1992**, *17*, 163.
(3) Fujishige, S.; Koiwai, K.; Kubota, K.; Ando, I. *Kenkyu Hokoku-seni Kobunshi Zairyo Konkyusho* **1991**, *167*, 47.
(4) Zhang, J.; Pelton, R. *Langmuir* **1996**, *12*, 2611.
(5) Zhang, J.; Pelton, R. *Colloids Surf.* **1999**, *156*, 111.
(6) Hua, X. Y.; Rosen, M. J. *J. Colloid Interface Sci.* **1988**, *124*, 652.
(7) Van Eijk, M. C. P.; Cohen Stuart, M. A. *Langmuir* **1997**, *13*, 544.
(8) Zhang, J.; Pelton, R. *Langmuir* **1999**, *15*, 8032.
(9) Kawaguchi, M.; Saito, W.; Kato, T. *Macromolecules* **1994**, *27*, 5882.
(10) Kawaguchi, M.; Hirose, Y.; Kato, T. *Macromolecules* **1996**, *12*, 3523.
(11) Elaisaaf, J. *J. Appl. Polym. Sci.* **1978**, *22*, 873.
(12) Schild, H. G.; Tirrell, D. A. *Polym. Prepr. (Am. Chem. Soc., Div. Polym. Chem.)* **1989**, *30*, 350.
(13) Wu, X. Y.; Pelton, R. H.; Tam K. C.; Woods, D. R.; Hamielec, A. E. *J. Polym. Sci., Part A: Polym. Chem.* **1993**, *31*, 957.
(14) Tam, K. C.; Ragaram, S.; Pelton, R. H. *Langmuir* **1994**, *10*, 418.
(15) Mears, S. J.; Deng, Y.; Cosgrove, T.; Pelton, R. *Langmuir* **1997**, *13*, 1901.
(16) Cabane, B.; Duplessix, R. *J. Phys. (Paris)* **1982**, *43*, 1529.
(17) Kwok, D. Y.; Vollhardt, D.; Miller, R.; Li., D.; Neumann, A. W. *Colloids Surf. A: Physicochem. Eng. Aspects* **1994**, *88*, 51.
(18) Clifton, B. J.; Cosgrove, T.; Richardson, R. M.; Zarbakhsh, A.; Webster, J. R. P. **1998**, *248*, 289.
(19) Penfold, J.; Thomas, R K. *J Phys.: Condens. Matter* **1990**, *2*, 1369.
(20) Gao, Y.; Au-Yeung, S. C. F.; Zhuo, S.; Wu, C. *J. Macromol. Sci., Phys.* **1997**, *B36* (3), 417.
(21) Purcell, I. P.; Lu, J. R.; Thomas, R. K.; Howe, A. M.; Penfold, J. *Langmuir* **1998**, *14*, 1637.
(22) Fleer, G. J.; Cohen Stuart, M. A.; Scheutjens, J. M. H. M.; Cosgrove, T.; Vincent, B. *Polymers at Interfaces*; Chapman and Hall: London, 1993.
(23) Kubota, K.; Fujishige, S.; Ando, I. Single-Chain Transition of Poly(*N*-isopropylacrylamide). *J. Phys. Chem.* **1990**, *94*, 5154; *Polym. J.* **1990**, *22*, 15.
(24) Richardson, R. M.; Cosgrove, T.; Eaglesham, A. *Langmuir* **1993**, *9*, 3530.
(25) Jean, B.; Lee, L.; Cabane, B. *Langmuir* **1999**, *15*, 7585.

MA000095P